LASER ABLATION OF ACTINIDES INTO AN ELECTRON CYCLOTRON RESONANCE ION SOURCES FOR ACCELERATOR MASS SPECTROSCOPY

T. Palchan[1], R. Pardo[1], F. Kondev[1], S. Kondrashev[1], C. Nair[1], R. Scott[1], R. Vondrasek[1], M. Paul[2], W. Bauder[3], P. Collon[3], G. Youinou[4], M. Salvatores[4,5], G. Palmotti[4], J. Berg[4], T. Maddock[4], and G. Imel[6]

[1] Physics Division, Argonne National Laboratory, 9700 S. Cass Avenue, Argonne, IL 60439 USA
[2] Racah Institute of Physics, Hebrew University, Jerusalem 91904, Israel
[3] Nuclear Structure Laboratory, University of Notre Dame, Notre Dame, IN 46556, USA
[4] Idaho National Laboratory, 2525 Fremont Avenue, Idaho Falls, ID 83415
[5] CEA-Cadarache, 13108 Saint-Paul-lez-Durance, France
[6] Idaho State University, 921 South 8th Avenue, Pocatello, ID 83209

Abstract

A project using accelerator mass spectrometry (AMS) is underway at the ATLAS facility to measure the atom densities of transmutation products present in samples irradiated in the Advanced Test Reactor at INL. These atom densities will be used to infer effective actinide neutron capture cross-sections ranging from thorium to californium isotopes in different neutron spectra relevant to advanced fuel cycles. This project will require the measurement of many samples with high precision and accuracy. The AMS technique at ATLAS is based on production of highly-charged positive ions in an ECRIS followed by injection into a linear accelerator. We use a picosecond laser to ablate the actinide material into the ion source. We expect that the laser ablation technique will have higher efficiency and lower chamber contamination than sputtering or oven evaporation thus reducing 'cross talk' between samples. The results of off-line ablation tests and first results of an accelerated beam generated by the laser coupled to the ECR will be discussed as well as the overall project schedule.

INTRODUCTION

Advanced nuclear fuel cycles are currently under evaluation in order to assess their potential to cope with new requirements of radioactive waste minimization, optimization of resource utilization and reduced risk of proliferation. This assessment should account for several key features of the fuel cycle, such as irradiated fuel processing, innovative fuel development and fabrication, waste characterization and disposal. In some cases, the impact of nuclear data and of their associated uncertainties can be crucial in order to assess further exploration. The need for accurate data has been pointed out in recent studies devoted to Generation-IV systems, see e.g. [1]. The very high mass actinides can play a significant role in the feasibility assessment of innovative fuel cycles. As an example, the potential build-up of ^{252}Cf when recycling all transuranics in a light water reactor, leads to increased neutron emissions that could impact the fuel fabrication process [2]. As a consequence, the poorly known nuclear data of higher mass transuranics need to be significantly improved.

At present, there is some information on these isotopes, but up to now, there has been little emphasis on the quality of these data and very little reliable uncertainty estimations have been provided. This situation is due to the difficulty to make both integral and differential cross section measurements for these isotopes.

The MANTRA (Measurements of Actinides Neutrons Transmutation Rates with Accelerator mass spectroscopy) project objectives are to obtain valuable integral information about neutron cross sections for actinides that are important for advanced nuclear fuel cycles. The proposed work takes advantage of two experimental facilities: the neutron irradiation capabilities of the Advanced Test Reactor (ATR) at the Idaho National Laboratory and the Accelerator Mass Spectrometry (AMS) capabilities of the Argonne Tandem Linac Accelerator System (ATLAS) at Argonne National Laboratory [3].

In this paper we will concentrate on the requirements of the AMS program and the novel aspects, specifically the laser ablation, that is implemented at the ECR ion source to carry out this research project. The requirements placed on the AMS measurements to be performed at ATLAS are quite challenging. These challenges include high-precision isotope ratio measurements, minimization of cross-talk between samples, efficient use of milligram samples, and the processing of an unprecedented number of samples for a facility as complex as ATLAS. Unique element (Z) identification is desirable, but is not expected to be possible except for specific cases.

The measurement configuration for ATLAS uses the ECR-II ion source [4], significantly modified as discussed below, as the source of ions. After acceleration and deceleration (increasing the accelerator m/q resolution but keeping the ion energy within acceptance range of analytical elements) in the ATLAS linac to approximately 1 MeV/u, the actinide ions of interest are counted in the focal plane of the Fragment Mass Analyzer (FMA) [5].

*Work supported by … U.S. Department of Energy, Office of Nuclear Physics, under contract No. DE-AC02-06CH11357

ISBN 978-3-95450-123-6

Small Sample Size and Cross-Talk

A major feature of AMS is the ability to analyze small samples. At ATLAS the AMS activities are focused on samples of a few milligrams. For this project, an added complexity is the need to deal with many small samples. The smaller the samples, the less are the radiological problems associated with handling α-emitting actinides for ATLAS operation. The need to measure many small samples as quickly as possible pushes us to develop efficient sample changing techniques for the ECR source and material delivery techniques which minimize source contamination.

We believe the best approach for this situation is to develop laser ablation for the feeding of sample material into the source. With laser ablation a very small and controllable amount of sample material can be introduced into the source without introduction of extraneous material from the sample holder. Also the angular distribution of ablated material by laser irradiation tends to be strongly peaked around the normal to the surface [6] which is expected to improve the efficiency of capture of ions into the plasma and thereby reduce wall contamination. Finally, the form of the sample material (metal, oxide, etc.) is less critical than with the sputtering or oven technique.

The ECR-II source will also be equipped with a quartz liner. The quartz liner will keep the main body of the source relatively clean of actinides, thus simplifying clean-up. Furthermore, there is some operational evidence that cross talk among samples is reduced. This effect has been observed with other AMS projects at ATLAS [7]. A negative to using a quartz liner is that source performance, as measured by charge-state distribution and maximum beam intensity, is somewhat reduced. But the beam energy is limited by the bending power of the FMA system and use of high charge state ions is not required. A mass-to-charge ratio of ~8-9 will be quite adequate for these measurements.

LASER PARAMETERS

Laser ablation into an ECR source was first developed at ATLAS [8] and used as plasma diagnostic tool [9]. It has since been used by a number of other labs to explore the coupling of laser produced ions into an ECR source [10]. The technique has not been used routinely for ion production and requires development for this application. The controlled release of materials into the plasma by well-focused laser light will eliminate the significant material buildup often seen in the region of the oven throat or beside the sputter cones, two techniques widely used for sample feeding to the ECRIS. The inefficient, indiscriminate injection of material into the source with these older techniques not only reduces the overall sensitivity of the method but is a major source of cross-contamination between samples. Our experience with lasers in the past indicates that the laser ablation approach will be much cleaner, but must be shown to work for this application.

Laser ablation is a term used to describe removal of material by laser action and it is distinguished from evaporation in equilibrium conditions. In order to remove an atom from a solid by means of a laser pulse one should deliver an amount of energy that exceeds the binding energy of that atom. Therefore the absorbed energy density per atom in a laser-heated layer E_{abs}, should at least be comparable to the heat of vaporization in equilibrium;

$$E_{abs} = 2AF(t_p)/n_a l_s . \qquad (1)$$

here A is the absorption coefficient; F is the incident laser fluence, the energy per unit surface area during the pulse of duration t_p; n_a is atomic number density and l_s is the skin depth of the laser in the solid [11]. There are three regimes of laser ablation depending on the laser and target parameters: The thermal ablation, the non-equilibrium semi thermal ablation and the extreme non-equilibrium electrostatic ablation. In the thermal ablation the laser pulse is longer than the major relaxation routes in the irradiated material. Heat conduction and hydrodynamic processes cause the removal of the atoms from the solids. As a consequence the ablation is accompanied by the formation of a large heat- affected zone and throws out molten material [12]. The second regime, non-equilibrium and semi-thermal, is realized when electrons have enough time to transfer the energy to the lattice and the average energy of the ions (temperature) exceeds the binding energy but the distribution function is far from the equilibrium Maxwell distribution. In these conditions, the majority of ions escape the solid before the equilibrium distribution is established. The extreme ablation regime, electrostatic ablation, is completely non-equilibrium and non-thermal. This mode is realized when a short powerful pulse elevates average electron energy during the pulse in excess of the sum of the binding energy of the ions plus the energy necessary for the electron to escape from a solid. The lattice remains cold during the pulse. The energetic electrons escaping from a solid create a huge electrostatic field of charge separation, which pulls the ions out of the solid [13].

In order to avoid a flow of macroparticles or molten materials into the ECR ion source, we chose a laser with picoseconds pulse duration. The properties of the laser that we are using in this application are:

- λ =1064 nm
- 15 ps pulse width
- Repetition rate up to 400 Hz
- Pulse energy: variable, up to 5 mJ per pulse.
- Maximum, power of $3x10^8$W per pulse.

OFF LINE TEST SET UP AND RESULTS

For characterization of the laser and to acquire a better understanding of the laser ablated material coupling with the ECR ion source plasma we performed tests in an off line setup. The experimental set up is shown in Fig 1. A 4000mm focusing lens is placed at the entrance of a vacuum chamber to mimic the distances required at the ECR source. The result of the optical set up is a focal spot with a diameter of 450μm at the FWHM. The maximum laser intensity at the focal spot is $2x10^{11}$W/cm^2. An image of the focal spot is presented in Fig 1.

The laser-induced ablation creates a plasma plume which rapidly expands. Typically the plasma expansion

ISBN 978-3-95450-123-6

speed is in the order of 10^6 cm/sec. During a picosecond ablation the number of ejected species is about 10^{13}atoms/pulse. The ion flux is about 1% [14]. Using a faraday cup located at a distance of 15.8cm from a solid Ti target we extracted the ion velocity by means of time of flight technique. The calculated averaged ion energy is 40±10eV. For Ti the corresponding velocity is $1.2x10^6$cm/sec. In addition we measured the ablating rates for different materials [15].

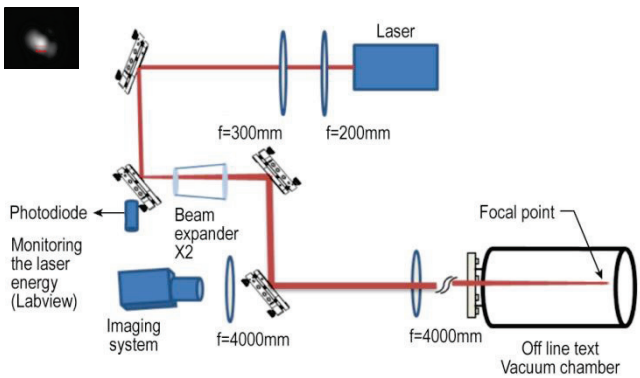

Figure 1: Off line test set up and the laser focal spot image.

These studies now provide us with the background information needed to better understand the laser/source performance when the laser is coupled to the ECR source.

INSTALLATION AT THE SOURCE

The installation of the laser at the source is shown in Fig. 2. The laser beam is delivered into the source through the extraction aperture. The ablation target is located at the rear of the ECR chamber near the edge of the plasma.

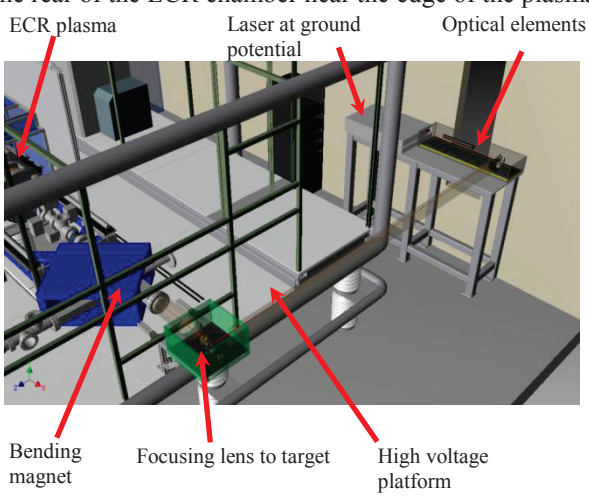

Figure 2: Drawing showing the laser ablation system relative to the ECR source HV platform.

Imaging of the Target Sample

In order to monitor the laser beam hitting the target samples, we developed an imaging system. The imaging system is located behind the last mirror that directs the laser beam into the source (see Fig 1). We installed a halogen light at the back of the iron taper, (see Fig 3). This way we can collect the scattered light behind the sample holder when it is in place. Using our imaging system we are able to image the outer edges of the sample holder. During a run, when the laser hit the sample we are able to identify where the laser hits the sample.

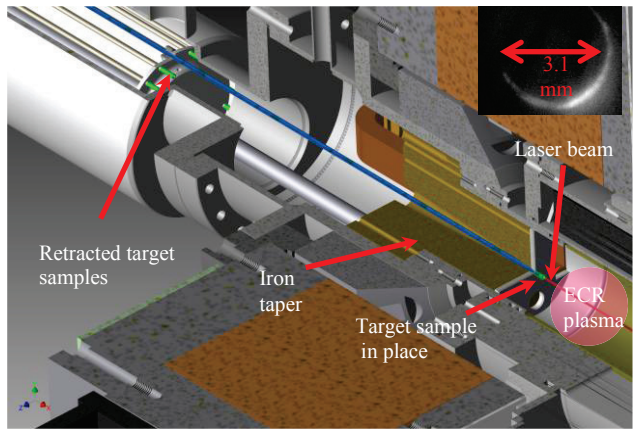

Figure 3: Multisample changer mounted on ECR source showing sample location with the back light.

Figure 3 shows the multisample changer interfaced to the source that we use in order to rapidly switch between the samples. See this proceeding for a detailed description of the multisample changer [16]. In addition the geometry of the laser beam relative to the plasma chamber is presented. The laser beam enters the plasma chamber on axis with the center axis of the plasma chamber. The target sample is inserted into the plasma chamber through the center of the bias disc.

ECR BEAM FROM ABLATED SAMPELS

Titanium Sample

Initial tests of the laser coupled to the ECR source took place with solid Ti sample. Fig 4 shows a Ti sample after irradiation. The laser parameters that we used during this test are 25Hz repetition rate and a variable energy of 0.5-1.5mj per pulse. The resulting peak intensity is $5x10^{10}$w/cm^2. The overall consumption rate was 0.3mg/hour.

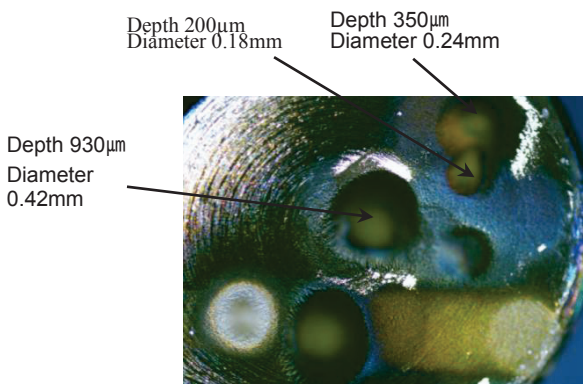

Figure 4: Ti sample after laser irradiations.

ISBN 978-3-95450-123-6

By means of laser ablation on a Ti sample we were able to generate a high charge state beam. The charge state distribution is shown in Fig 5. From the charge state distribution, it is clearly evident the beam production drops to a very low level of 0.1μA when the laser is off compared to 1μA when the laser is on.

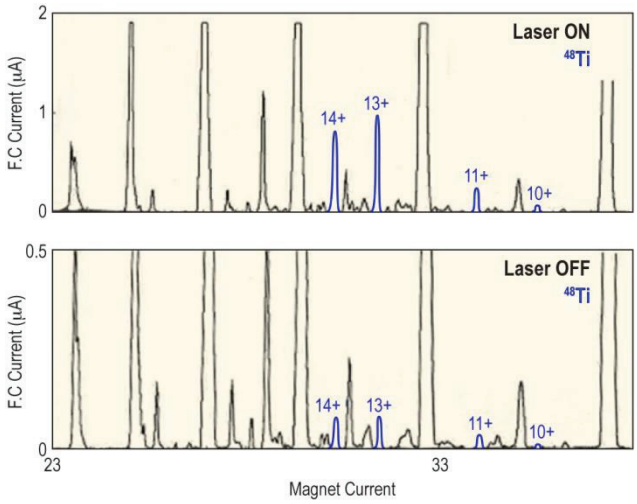

Figure 5: Charge state distribution of Ti beam. The Ti peaks are labeled with mass/charge state in the two figures. The charge–state distribution peaks at 13+. For sputter technique the charge–state distribution peaks at 10+-12+.

For long term stability (100minutes) we measured the $^{48}Ti^{13+}$ charge state. The laser energy that we used for those measurements was 1.5mj with 25Hz repetition rate. The laser beam diameter at the focal spot was 0.5mm. Fig 6 shows the faraday cup current trend with the corresponding laser energy. The generated beam is around 4 μA and stable for the first 10 minutes and then it drops by 80% for the next 20 minutes while on the same time the laser energy is stable. After that the beam stays stable at a lower level of 0.6 μA for more than an hour.

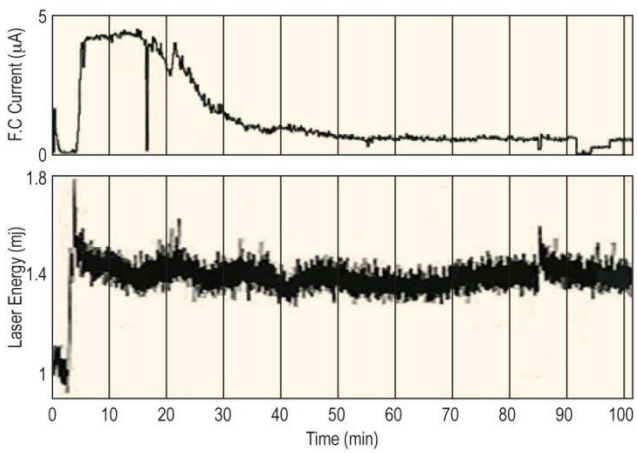

Figure 6: Long term of Ti beam and the corresponding laser energy for 0.5mm diameter in the focal spot.

One of the reasons for this beam current instability is the drilling rate of the laser in the sample.

Terbium Oxide Sample at the ECR Ion Source

In order to lower the drilling rate and to gain more stability we used a laser beam manipulator and moved the laser beam on the sample at a constant rate. The beam manipulator consists of two controlled motors that are connected to the aligning knobs of the last mirror that sends the beam into the vacuum chamber (see figure 1). The minimal step size on the target using the beam manipulator is 110μm.

In this test we used a terbium oxide powder as a sample. The powder was packed into one of the multisample changer holder. The laser parameters in this test were100Hz repetition rate and energy of 2.3mj per pulse. The overall consumption rate was 0.32mg per hour. Figure 7 shows the time dependence of the $^{145}Tb^{24+}$ charge state. From the term it is evident that there is a periodic pattern in the beam production. This periodicity is attributed to the pattern of the laser beam raster. The beam was moving over a region of 0.36mm^2.

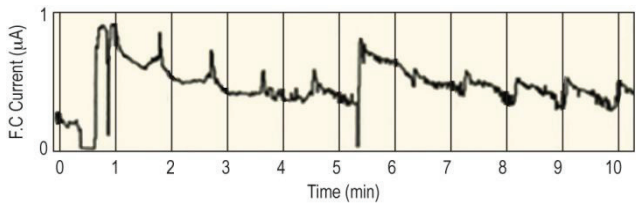

Figure 7: Tb beam time dependence with a constant rate moving of the laser beam on the sample.

Figure 8 shows the charge state distribution of the Tb beam produced by means of laser ablation.

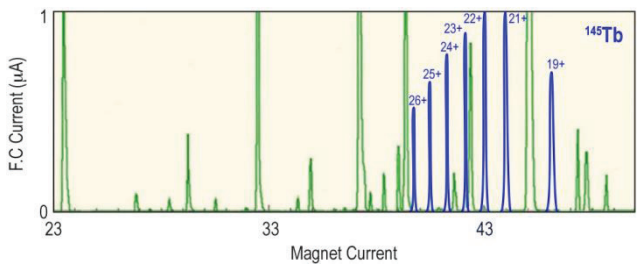

Figure 8: Charge state distribution of Tb beam. The Tb peaks are labeled with charge state. The charge–state distribution peaks at 22+.

Aluminum Sample

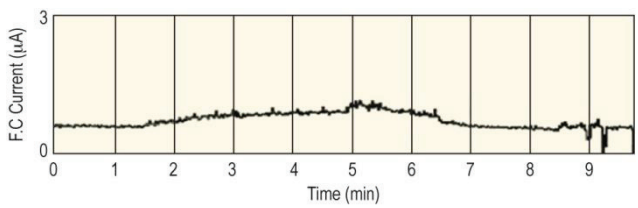

Figure 9: Term of Al beam with a constant sweep rate of the laser beam on the sample.

After some adjustment with the raster pattern of the laser beam (we reduced the moving region to be 0.2mm^2) we were able to stabilize the beam production. Figure 9 shows the beam production of $^{27}Al^{8+}$ where the periodic pastern is gone but the overall production is low. The

ISBN 978-3-95450-123-6

laser parameters in this test were100Hz repetition rate and energy of 2.2mj per pulse. The overall consumption rate was 0.45mg per hour.

Uranium Oxide Sample

The uranium oxide powder was packed also to one of the multisample holders. In this test the laser parameter were 200-400Hz repetition rate and energy of 5mj per pulse. Figure 10 shows the charge distribution of the uranium ion beam. The overall consumption rate was 0.7mg per hour. We were not able to measure the beam long term because the production of the beam was neither high enough nor stable.

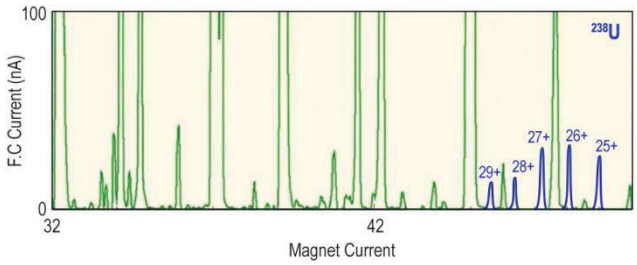

Figure 10: Charge state distribution of Uranium.

NEW DESGIN FOR THE SAMPLE LOCATION

During the tests we noticed that the source performance even without the laser ablation were low and unstable. The production of $^{16}O^{6+}$ beam (oxygen is the supporting gas) was 35μA compared to 160 μA under similar conditions. After some investigation we came to the conclusion that the missing bias disc at the center axis of the plasma chamber has a significant effect on the ECR ion source performance. The production of $^{16}O^{6+}$ beam was restored to normal levels with the disc filled with Al at the center. Therefore we are redesigning the injection system in order to move the location of the sample target to be 0.3 inches off the center. This way the bias disc center is solid aluminum where most of the plasma hits. The hole in the disc is not interfering with the performance of the source. Also this may further reduce the beam from the sample when the laser is turned off. We tested the source with the new location for the hole in the bias disc and got the same results as with the complete bias disc.

CONCLUSIONS

We have demonstrated high charge state beams generated at the ECR source from laser ablated material. To improve the production of the generated ion beam we plan to move the sample location to be off axis. In addition we plan to investigate the influence of the spatial beam profile, especially a flat top profile, on the production of the ion beam.

REFERENCES

[1] M.Salvatores, "Nuclear Data for Advanced Fuel Cycles", Proc. Int. Conf. IEMPT-10, Mito, Japan, 6-10 October 2008.
[2] G.Youinou, et al., INL/EXT-09-16091, 2009; http://www.inl.gov/technicalpublications/Documents/4282336.pdf.
[3] G.Youinou, et al., “An Integral Reactor Physics Experiment to Infer Actinide Capture Cross-Sections From Thorium To Californium With Accelerator Mass Spectrometry”, Eleventh International Conference on Nuclear Data for Science and Technology, Jeju Island, Korea, 2010.
[4] M. Schlapp, et al.,"A new 14GHz electron-cyclotron-resonance ion source for the heavy ion accelerator facility ATLAS” Rev. Sci. Instrum. 69 (1998) 631.
[5] C.N. Davids, et al., “Startup of the Fragment Mass Analyzer at ATLAS”, Nucl. Instrum. and Meth. B 70, 358(1992).
[6] S. Mao et al., “Initiation of an early-stage plasma during picosecond laser ablation of solids” Appl. Phys. Lett. 77, 2464 (2000).
[7] M. Gaelens, et al., Rev. Sci. Instrum. 75, 1916 (2004).
[8] R. Harkewicz, et al., Rev. Sci. Inst. **65**(4), 1104(1994).
[9] R C Pardo, et al., Rev. Sci. Inst. **75** (5), 1427(2004).
[10] S. Gammino, et al., J. App. Phy. **96** (5), 2961 (2004).
[11] E.G.Gamaly, “The physics of ultra-short laser interaction with solids at non-relativistic intensities” Phy. Reports. **508** 91 (2011).
[12] S. Nolte et al., “Ablation of metals by ultrashort laser pulse” J. Opt.Soc. Am. B **14** (10)2716(1997).
[13] P.T. Mannion, et al., “Langmuir probe investigation of plasma expansion in femto-and picoseconds laser ablation of selected metals” J. of Phy :Conference series **59** 753 (2007). Conference on Laser ablation (COLA'05) Banff, Canada 2005.
[14] W. Marine, et al.,”Laser induced plasma formation by picoseconds pulse irradiation” Appl. Surf.Sci. **69** 290 (1992).
[15] T.Palchan, et al., HIAT2012, Chicago, Illinois (2012), TUC03, to be published.
[16] R.Vondrasek, et al. “A multi sample changer coupled to an ECR source for AMS experiments” these proceeding.

ISBN 978-3-95450-123-6